ELECTROPHORETIC DEPOSITION OF OXIDIZED MULTI-WALLED CARBON NANOTUBES ON STAINLESS STEEL FOR LPG SENSOR

A DISSERTATION

SUBMITTED FOR THE PARTIAL FULFILLMENT OF THE REQUIREMENTS FOR THE MASTER OF SCIENCE DEGREE IN CHEMISTRY

BY

Rima Chaudhary

Exam Symbol No.: 467/072

T.U. Reg. No.: 5-2-0037-1149-2011

SUBMITTED TO

CENTRAL DEPARTMENT OF CHEMISTRY

INSTITUTE OF SCIENCE AND TECHNOLOGY

TRIBHUVAN UNIVERSITY KIRTIPUR,

KATHMANDU, NEPAL

September 2023

BOARD OF EXAMINER AND CERTIFICATE OF APPROVAL

This dissertation entitled "**ELECTROPHORETIC DEPOSITION OF OXIDIZED MULTI-WALLED CARBON NANOTUBES ON STAINLESS STEEL FOR LPG SENSOR"** by Mrs. Rima Chaudhary under the supervision of Assoc. Prof. Dr. Sabita Shrestha, Central Department of Chemistry, Tribhuvan University, Kathmandu, Nepal, is hereby submitted and has been approved for the partial fulfillment of the Master of Science (M. Sc.) Degree in Chemistry.

……..

Supervisor

Assoc. Prof. Dr. Sabita Shrestha

Central Department of Chemistry

Tribhuvan University, Kirtipur

……..

Internal Examiner

Prof. Dr. Megh Raj Pokhrel

Central Department of Chemistry

Tribhuvan University, Kirtipur

…….……

External Examiner

Assoc. Prof. Dr. Sharmila Pradhan

Amrit Science Campus

Tribhuvan University, Kathmandu

…..……..

Prof. Dr. Jagadeesh Bhattarai

Head,

Central Department of Chemistry

Tribhuvan University, Kirtipur

September 2023

RECOMMENDATION LETTER

This is to certify that the dissertation work entitled **"ELECTROPHORETIC DEPOSITION OF OXIDIZED MULTI-WALLED CARBON NANOTUBE ON STAINLESS STEEL FOR LPG SENSOR"** submitted by Mrs. Rima Chaudhary for the Degree of M. Sc. in Chemistry of Tribhuvan University was carried out under my supervision in the academic year 2016-2023. During the research period, Mrs. Rima Chaudhary had performed the work sincerely and satisfactorily.

…….

Supervisor

Assoc. Prof. Dr. Sabita Shrestha

Central Department of Chemistry

Tribhuvan University, Kirtipur

Kathmandu, Nepal

September 2023

DECLARATION

I, *Mrs. Rima Chaudhary*, hereby declare that the work presented that the work presented herein work and done originally by me and has not been published or submitted elsewhere for the requirement of a degree program. Any literature, data or works done by others and cited in this dissertation has given due acknowledgement and listed in the reference section. This dissertation work has not been submitted to any other degree in this institute.

…….

Rima Chaudhary

September 2023

DEDICATION

(Dedicated to my parents)

ACKNOWLEDGEMENTS

I would like to express my sincere gratitude to my research supervisor Assoc. Prof. Dr. Sabita Shrestha, Central Department of Chemistry Tribhuvan University Kirtipur, for her valuable guidance, support and suggestion throughout this research work.

I am obliged to head of the Department, Prof. Dr. Jagadeesh Bhattarai and former Heads Prof. Dr. Ram Chandra Basnyat and Prof. Dr. Megh Raj Pokhrel, Central Department of Chemistry, Tribhuvan University, for providing me an opportunity to conduct my thesis work at Central Department of Chemistry T.U. I would also like to thank all the faculty members of department from the bottom of my heart for their guidance and knowledge with which I have been ventured so far.

At last, but not the least my undying love and gratefulness goes to my beloved parents Mr. Ram Das, Mrs Shyamlali Devi, my brother Manoj who have unconditionally guided, supported and tolerated me so far.

Rima Chaudhary

September 2023

ABBREVIATIONS

EPD	: Electrophoretic Deposition
CNTs	: Carbon Nanotubes
NPs	: Nanoparticles
SWCNTs	: Single Walled Carbon Nanotubes
MWCNTs	: Multiwalled Carbon Nanotubes
EDL	: Electrical Double Layer
PTEF	: Promising Technique for massive Fabrication Electrode
SEM	: Scanning Electron Microscopy
FTIR	: Fourier Transformation Infrared Spectroscopy
DC	: Direct Current
AC	: Alternating Current
CVD	: Chemical Vapor Deposition
^{o}C	: Degree Celsius
mm	: Multi-meter
SDS	: Sodium Dodecyl Sulphate
nm	: Nanometer
R_a	: Resistance in presence of air
R_g	: Resistance in presence of gas

ABSTRACTS

This dissertation research describes the feasibility study and investigation of Electrophoretic Deposition of oxidized MWCNTs on stainless steel for LPG sensor. Gas sensors are attracting tremendous interest because of their wide spread application in industry, environmental monitoring, space exploration, biomedicine and pharmaceuticals. Gas sensors with high sensitivity and selectivity are required for leakage detection of explosive gases such as hydrogen, and for real time detection of toxic and pathogenic gases in industries. There is also a strong demand for the ability to monitor and control our ambient environment, especially with the increasing concern of global warming. MWCNTs are used to obtain thin film by Electrophoretic Deposition. Before deposition MWCNTs were purified and surface functionalized by conc. HNO_3. The oxidized MWCNTs were characterized by FTIR. FTIR shows the presence of oxygenated functionalized groups as carboxylic acid and hydroxyl group on the surface of MWCNTs. The uniform Electrophoretic deposition of MWCNTs are confirmed by SEM. Raman spectroscopy confirmed the deposited material was MWCNTs.

The EPD experiments were carried out by using oxidized MWCNTs on stainless steel plate at 10V at a constant time of 10 min. and fix electrode distance of 1.5 cm. Modification of carbon nanotubes with functional groups will greatly enhance the selectivity of the carbon nanotubes-based gas sensors have proved to work well at room temperature, which reduces power consumption of the device and enables the safer detection of flammable gases. The resistance of Electrophoretic deposited material was measured in closed glass chamber with digital multimeter. Then % sensitivity was calculated. It was observed that the rate of sensitivity increases with time and become constant after certain time.

Keywords :

LPG sensor, Carbon nanotubes, Electrophoretic deposition, sensitivity, Oxygenated

TABLE OF CONTENTS

LIST OF FIGURES

CHAPTER-1

INTRODUCTION

1.1 Nanotechnology

The branch of science which studies about the preparation of nanoparticles having specific morphologies and properties which studies materials whose size lies within the nanometer range between 1 to 100 nm ($1nm=10^{-9}m$) [1]. Among all complications, the well known Professor Mr. R. Feynman of California institute of technology conveyed the lecture at the meeting of the American Physical society termed as, "There is a lot of space down there." In 1959, for the first time the probability to design nanosized products with the use of atoms as fabrication particles. This lecture is concerned as the origin of the nanotechnological pattern in current days. Later, E Drexler expanded ideas of nanotechnological grand design and redirected by Feynman in his book "vehicles of creation": the advent of nanotechnological time bring out in 1986 [2].

It is an associative field of physical chemistry engineering, environmental and biological sciences explain with various types of nanoparticles [3]. Nanoparticles

are of various kinds on the basis of their size morphology, physical properties like ceramic nanoparticles, metal nanoparticles, polymeric nanoparticles, lipid based nanoparticles [4].

1.2 Carbon Nanotubes

CNTs were initially stumble in 1991, by Sumia inside fullerene black. Here, C-atom is arranged in tubular form on a miniature level. CNTs are coaxial cylinders of graphite sheets. The first observation Sumio made were of MWCNTs were observed. In 1996, Smally prepared bundles of SWCNTs for first time.

1.3 Synthesis of CNTs

There are various methods for the preparation of CNTs like Arc growth, Condensation Vaporization Densation (CVD), Catalytic Decomposition of

hydrocarbons, heat treatment of polymer, low temperature pyrolysis, Catalytic chemical vapor deposition etc.

Among them, most alluring profitably used method is CVD. The fundamental mechanism of this method is the decomposition of hydrocarbon molecules. The structure of CNTs synthesized by Chemical Vapor Deposition technique depend on the operating condition like temperature, pressure, volume and concentration of CH_4.

1.4 Types of CNTs

On the basis of number of grapheme layers, CNTs are of two types

a) SWCNTs that is made up of honey comb matrix of C-atoms that can be pictured as circular solid folded from a graphitic sheet.

b) MWCNTs that are made up of a multiple rolled layers of graphite circular solids normally split up by a flat capacity of graphite.

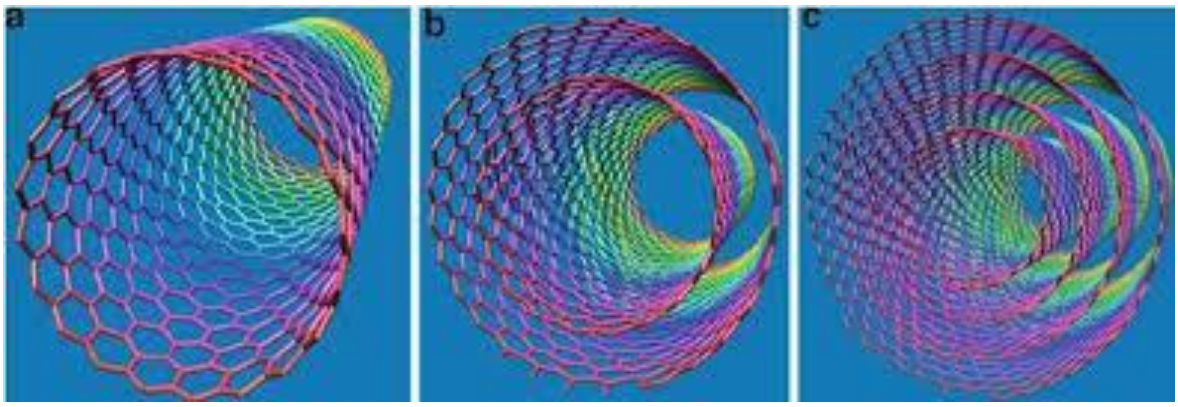

Fig. 1.4: Images of single, Double and multi-walled CNTs

1.5 Applications of CNTs

CNTs are stunning nanostructures that have been extensively explained and researched. Due to amazing electronic and mechanical properties, large number of areas were explored. It covers microelectronic devices, , hydrogen storage, quantum wires, etc [5].

1.6 Electrophoretic Deposition (EPD)

1.6.1 Definition

Electrophoretic deposition is an electrochemical technique achieved in two electrode cell. If direct current is supplied, charged fragment present in a relevant liquid move towards the respective electrodes. So, the fragments assemble at the settling electrode and design comparatively dense and similar films. This method is exceedingly pliable when colloidal interruption of glass, ceramics can be properly conducted by electrophoretic deposition. In fact, steady suspensions can be electrically charged and collected. But the substrate must be contributive/varnished by a conductive film. Furthermore, the coating features can be easily enhanced by managing the deposition factors. Among other techniques such as coating, thickness curb and nanopowder usage are easier with electrophoretic deposition [6].

Due to the broad employment of EPD in many industries, it has highly flexible implementation, queit equipment, short operating time, cost effectiveness, superficial moderation. It is applicable for academia as well as industry due to production of best quality of microstructure, geometrical shapes etc. Aqueous EPD is commercially used. However, non-aqueous EPD applications are known [7].

As a first example of EPD experiment, Manrique has varnishes Ti_6Al_4V substrates with bio-glass powder by the process of EPD, afterwards followed by a suitable heat treatment to constrict the coating. Plane imperfection- free thick (greater than 1 nm) fabricating were formed on anodized Ti_6Al_4V cylindrical surface. EPD parameters were enhanced to form coating with desired thickness [8].

1.6.2 Fundamental Concept of Electrophoretic Deposition

EPD is a method used for coating of charged fragments in a steady viscous solution on a conductive substrate. The fabricated fragment from the deliberate materials [5]. Both AC as well as DC are applicable in electrophoretic deposition method. Inspite of direct current fields are more usual. EPD qualifies coating of vast dimensions from spongy platforms to highly dense coating. These structures cover various components with complex shapes and structures [9-11].

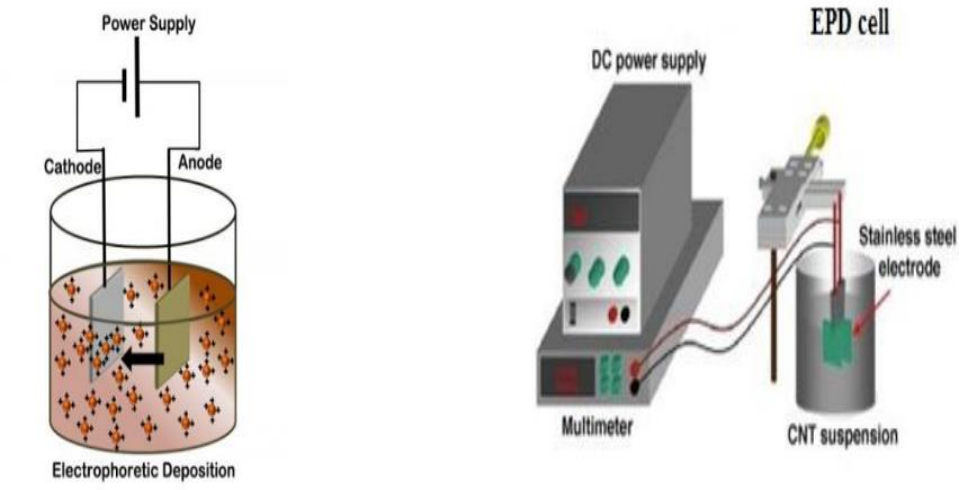

Fig.1.6.2 Schematic diagram of Electrophoretic Deposition Process

1.7 Types of EPD

On the basis of polarity of electrodes, there are two types of EPD.

1.7.1 Anodic Electrophoretic Deposition

The EPD in which the negatively charged particles deposited on the positive electrodes.

1.7.2 Cathodic Electrophoretic Deposition

The EPD in which the positively charged particles deposited on the negative electrodes, it is called cathodic electrophoretic deposition.

Hence, by suitable modification of the surface charge on the particles, any of the two types of depositions are possible [12].

1.8 Factors affecting EPD

Two categories of criterion resolve the features of this method.

1.8.1 Parameters Linked to the Suspension

- **Fragment size**

  There is no rule for EPD process. A good deposition occur in the range of 1-30 μm [13].

- **Dielectric Constant**

  Capacity about material to stock electrical energy in applied field is termed as electric field. Toppling stops at very small dielectric constant. But at high value, minimizes the dimensions of binary coating field and finally reduces the electrophoretic motion. So, low dielectric constant is more suitable for EPD [14].

- **Conductivity of Suspension**

  The movement of particle is too slow when the interruption is very conductive. However, for very resistive interruption, electrically the particle being charged as well as the firmness is lost. Appropriate conductivity is various materials and systems [15].

- **Viscosity of Suspension**

  Suspension with low viscosity indicates a good EPD.

- **Zeta Potential**

  It is the charge which develops at the junction among a solid surface and it's liquid medium. This potential is measured in millivolts. It is the main index of the firmness of colloidal distributions. It shows the electrostatic aversion among adjoining, similarly charged fragment in distribution. Higher the infinite value of zeta potential the superior distribution of fragments [16].

  When absolute value of zeta potential is < 25 mV, the repellent force don't the exceed the Van der waals allurement among fragment. So, the fragment start to aggregate. To neglect this, high electrostatics aversion caused by high particle charge is enforced [17].

- **Stability of Suspension**

Generally, a well-dispersed stable suspension will provide a better deposition during EPD process compared to an unstable or agglomerated powder suspension.

1.8.2 Parameters Related to the Process

(a) Deposition Time

Deposition time always maintain in the EPD process. It should be fixed. Deposition time is directly proportional to the thickness will be obtained i.e., deposition rate increases with increase in deposition time [18].

(b) Applied Voltage

Applied voltage in EPD is precisely proportional to the amount of deposition. It is noted that, at 25-100 V/cm uniform and homogeneous, but at >100 V/cm, deposition quality is decreases. [19].

(c) Concentration in Solid of Suspension

Generally, higher toppling rate is anticipated with increase in fragment concentration.

(d) Conductivity of Substrate

It is used for comparing the grade of toppling by electrophoretic deposition. It has been noted that low conductivity results in non-uniform and low deposition of films compared to higher.

(e) Electrode Separation

It can be observed that, closer the distance between electrodes, higher the thickness of the films is predicted [20].

1.9 Mechanism of Electrophoretic Deposition

1.9.1 Flocculation by Particles Accumulation

The process of EPD was completed by Hamaker and Verwey. They concluded that the construction of deposits by electrophoresis is parallel to the configuration of residue payable to gravitation. The basic purpose of the applied electric field in EPD route is to compel the fragments towards the aim electrode and aggregate close to it [21].

1.9.2 Particle Charge by Neutralization Mechanism

The particles engage in charge neutralization depend on contact with the deposition electrode as well as applicable for single particles or monolayer deposits.

It describes the coating of powders that are charged caused by salt solution [22]. However, this phenomenon is unreasonable for succeeding situations

i) EPD for long time (thickness deposites)

ii) While particles electrodes operations are prohibited

iii) p^H shifting electrochemical reactions close/near electrodes.

1.9.3 Electrochemical Particle Coagulation Mechanism

The present operation indicates fall of revolting forces among fragments that cause coagulation. Inter particles revulsion decreases and finally coagulation appears because of enhance of electrolyte attentiveness as explained via Koelmans [23]. This mechanism is true when electrode reactions produce OH^-. However, this method is infirm with increment of electrolyte concentration close to electrode.

1.9.4 Electrical Double Layer Distortion Thinning phenomenon

Sarkar along with Nicholson provided the clarification for particles coating phenomenon while there is no raise of electrolyte attention close to the electrode by allowing for the motion of positively charged oxide fragment in the direction of the cathode in EPD compartment. The anticipated mechanism of this model is [24].

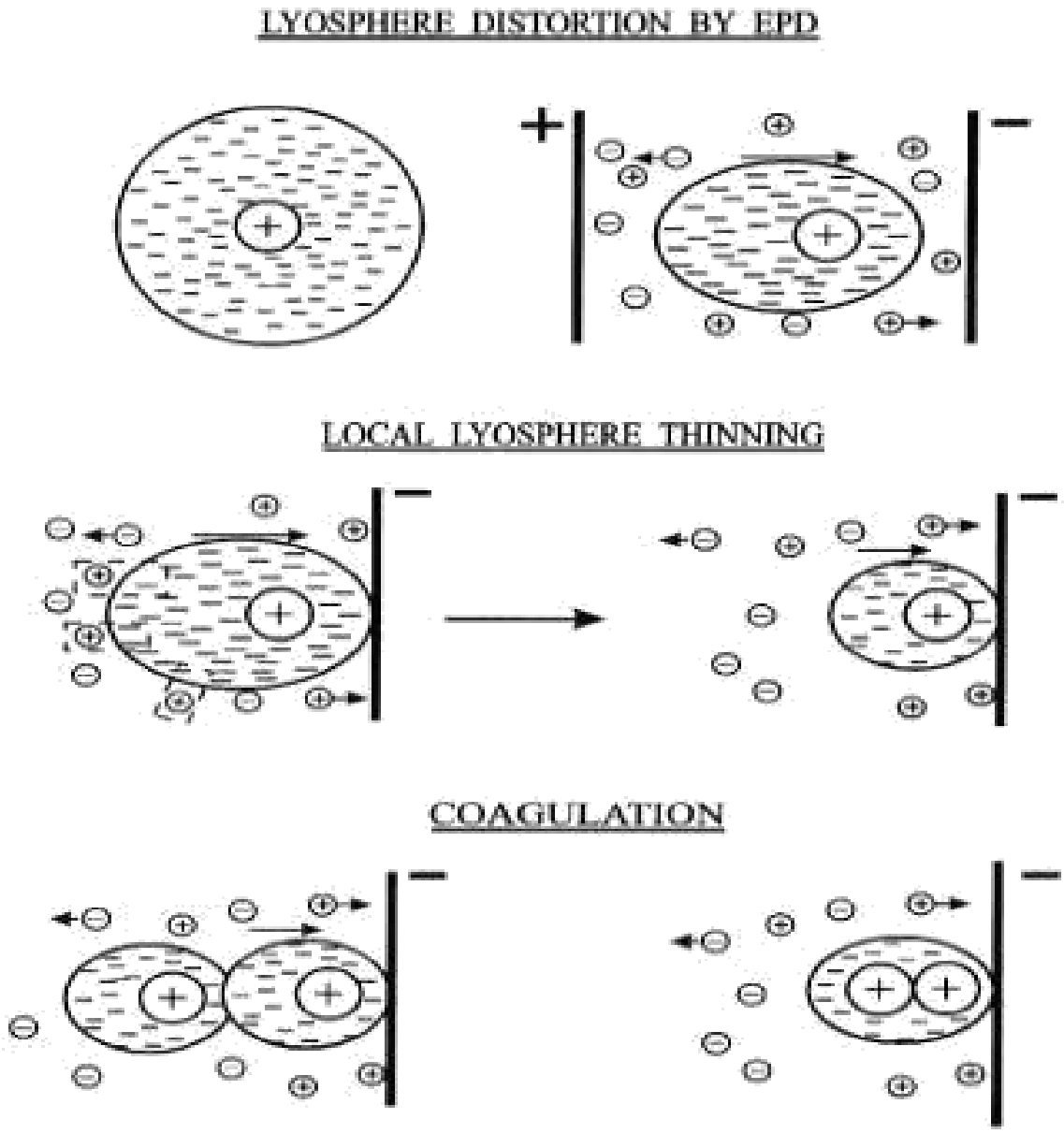

Fig.1.9.4 Schematic diagram of EDL and thinning Mechanism for EPD process

1.10 LPG Sensor

LPG is hydrocarbon compounds containing propane and butane. It is broadly used as a burning equipment. In addition, LPG is of major risky because of its inflammable, explosive nature. To keep away from the harm caused by leakage as well as gas explosions, it is crucial to identify its leakage [25]. Metal oxide semiconducting equipments are significantly applied as LPG sensor [26-27]. To defeat such boundaries, production of LPG sensor operated at normal temperature has obtained core significance [28-29]. Several articles provides on the expansion of LPG sensors that work at ordinary temperature, the decline of the MOS size [30-31], and the mixing of MOS with metal NPs [32] consisting the fabrication of hetero junctions [32-34], which is one of the most scenario used. Variation in resonse of sensor are gained by mixing of MOS with NPs [35]. Additionally, produced junction potential at boundary among MOS in addition to further nanostructured equipments has also increased the response achievement for sensor [36-38]. Hence, additional reports for coating tools based on hetero junctions are required, particularly in microstructure systems.

1.11 Applications of EPD

1.11.1 Oriented Ceramics Materials

Electro deposition is developing a principal technique in ceramic clarification. The EPD allows the development of thin ceramic films. EPD is an important device in developing thick ceramic films. For the coating of crystalline oriented thick films, it has been noted that EPD is an encourazing device [39].

1.11.2 Multilayered Composites

Due to more validity of EPD, it is also efficient for the coating of functionally gradient and multilayer composites [40].

1.12 Sensors

Gas sensors are impressing enormous attentiveness due to their extensive implementation in industry, environmental consideration, territory investigation as well as pharmaceutics. Gas sensors having elevated sensitivity and selectivity are

necessary in support of escape detection of volatile gases as well as in support of actual instant detection of harmful gases in manufactory. Additionally, a tough stipulate for the capacity to check as well as manage normal environment, i.e. global warming. Investigators from NASA explored the utilization of best-execution gas sensors in favor of identification of impressive elements of diverse planets. Additionally, nerve agent sensing meant for home safety is too at the centre about civic interest [41].

1.13 Application in LPG Sensor for Measurement of Electrical Resistance

In this process, the electrical resistances of the sensors would be measured at ordinary temperatures. Sensor response would study in a sealed glass chamber. The target gas will pass and the resistance will be measured. The chamber was restored and the experiments would replicate [42].

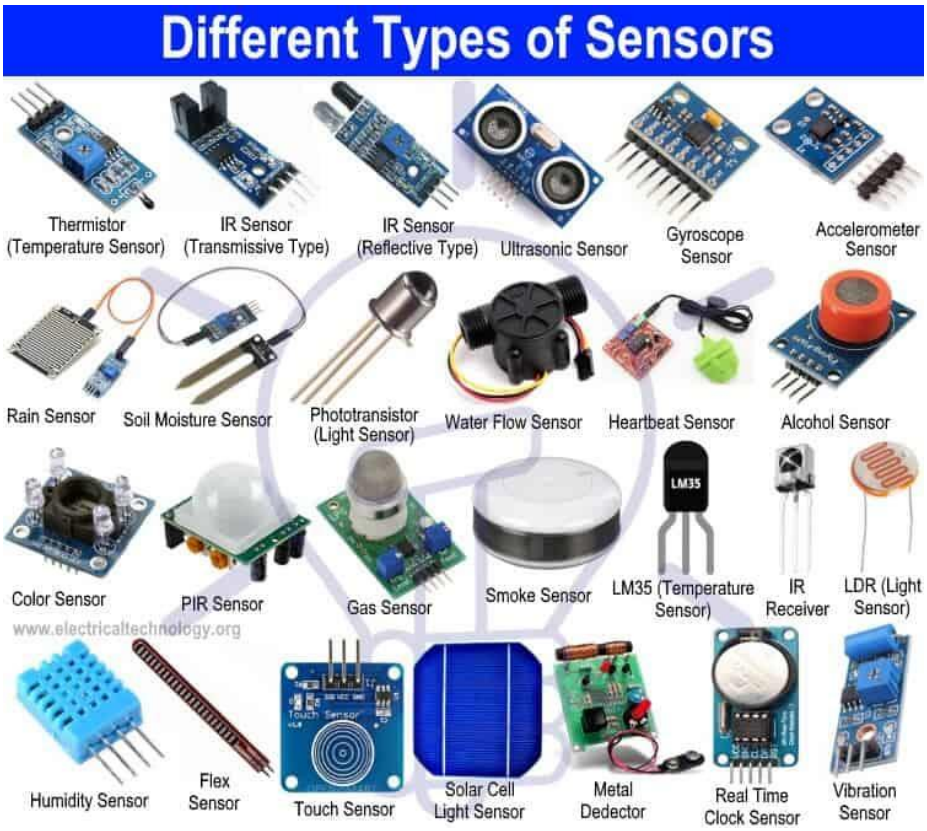

Fig 1.13 Different models of sensors

CHAPTER-II

OBJECTIVES OF THIS STUDY

❖ **General Objectives**

The principal intention of this work is electrophoretic deposition of oxidized MWCNTs on stainless steel for LPG sensor.

❖ **Specific Objectives**

- Purification and oxidation of MWCNTs.
- EPD of oxidized MWCNTs on the stainless steel plate.
- It's application in LPG sensor.

CHAPTER-III

LITERATURE REVIEW

There is a long history of research on about the LPG sensor by using different materials. Some of them are recapitulated below:

Shinde *et al.* successfully prepared ZnO thin film by Chemical Bath Deposition (CBD) technique using aq. $Zn(NO_3)_2$. The prepared films were characterized by SEM and XRD. SEM declared, zinc oxide films were of hexagonal in shape developed upright to substrate phase. XRD affirmed the structure of ZnO is wurtzite, is highly oriented along (002) plane compared to other plane (100 and 101). The sample coated at 80 min. (C_2) showed better response than other sample C_1 (60 min.) and C_3 (100 min). The maximum response 28% at 673K was noted on exposition of 10% of LPG for C_2. The prepared film also revealed good sensitivity and fast response-recovery features of liquefied petroleum gas [43].

Kasim *et al.* successfully manufactured nano-structured ZnO- MWCNTs by chemical route at ambient temperature. The prevalence about ZnO-nanoparticles inside the multi-walled carbon nanotubes were confirmed with XRD, UV- Visible spectroscopy, SEM and TEM. They show maximum transmission in the visible region [44].

Dangi *et al.* successfully studied and characterized the MWCNTs oxidized by reflux method using conc. HNO_3. The Ni-decorated oxidized MWCNTs on stainless steels were deposited by EPD process due to simple and cost-effective. The coated films were characterized by FTIR, SEM and EDX. The Ni-nanoparticles were coated on the surface of oxidized MWCNTs by wet chemical route using ethylene glycol as reducing agent. The Ni-decorated MWCNTs were used for production of hydrogen gas via alkaline electrolysis using NaOH as electrolyte dur to simple and easiest method [45].

Machappa *et al.*, demonstrated that gas sensing feature of PANI/$MgCrO_4$ composites. These complex were prepared by in situ polymerization. Variant in resistance is due to enhance concentration of gas in sensing sample. The response time for saturation is 17 min. The PANI/$MgCrO_4$ shows a proficient sensing stuff in support of LPG [46].

Ghos *et al.* found that ZnO fabric were developed on glass substrates. SEM verify the steady coating. For heated films, optical band was 3.14 eV. The higher sensitivity towards LPG at optimized temperature of 200℃ was manifested by sensor[47].

Akbarzadeh *et al.* investigated that TCVD growth of multi-walled carbon nanotubes were noted through catalytic decay of LPG at 580-800℃. SEM and TEM signify curved structure and dense morphology. Crystal quality is proportional to growth temperature. CNTS produced have smaller diameters. [48].

Aarthy *et al.* found that virulent and inflammable gas revelation acts as a key function in environmental air essence examination. Pt-NPs were conveyed scheduled sensing medium to enhance the sensor presentation. Important enhancement in response of Zn_2SnO_4 on zinc oxide nanorods was noticed [49].

Patil *et al.*found that nonostructured hollow spheres of SnO_2 were prepared through Ultrasonic atomization. Heavy fabric sensors were coated by curtain engraving method. High response (1990) is observed at 350℃[50].

Gurav *et al.* found that numerous ZnO micropattern are integrated by chemical technique. ZnO micropatterns significantly affect LPG sensing properties. Additionally, increased response is attained for vertically aligned ZnO rods. It is the best path to form super class ZnO films for efficient LPG sensor [51].

Nemade *et al.* found that the addition of grapheme into Bi_2O_3QDs, makes grapheme surface defective. This directly and simply confirmed using fluorescence spectroscopy. Simultaneously, provide strong support to improvement in LPG sensing properties based on defect density. The 80 wt.% grapheme/Bi_2O_3 composite possesses high sensing response, low operating temperature, fast response and recovery time along with good stability are adequate to be a practical LPG sensor. Low operating temperature feature of 80 wt.% graphene/Bi_2O_3 composite chemiresistors reduced the operation cost as well as risk [52].

Ravikiran *et al.* found that PANI and PANI-CMC complex have been prepared through chemical polymerization technique. XRD indicates a shift in d-spacing of PANI ensuing in superior p-electron delocalization. SEM studies of the composite show the presence of nanosize particles more densely packed as against micron size

of PANI particles. Complex plane impedance plots and their simulations for pristine PANI and PANI-CMC composites show a single semicircle obeying Debey's model. But plot for the composite has an additional RC element thus confirming the role of CMC in the composite. Apart from it's role as a composite, CMC also acts as a dopant which is advantageous as far as process ability of PANI is concerned as it avoids complex doping techniques saving cost and time. An important result from the LPG sensing studies is that the sensitivity of the composite is high compared to pristine PANI. Studies on it's stability, recovery and response time have shown that the composite has the potential to become an efficient LPG sensing device operable at room temperature besides being cost effective and easily processable [53].

Patil *et al.* demonstrate that PANI and PANI/ZnO complexes be profitably coated by via electro spinning method. SEM depicts that the clear nanomaterials of As-incorporated PANI as well as PANI/ZnO films. PANI/ZnO film indicates rapid response as well as recovery than pure PANI composite. Hence, PANI/ZnO is superior entrant for LPG perception at ambient temperature [54].

Jaiswal *et al.* reported that the successfully synthesized and characterized bimetallic Cu/Pd nanostructures. The topography of the sensing film reveals a porous morphology and also developed a simple and effective strategy to fabricate a sensor (humidity and LPG) by meso-porous Cu/Pd bimetallic nanostructured thin film. The sensitivity of the sensor was measured over an LPG concentration range from 1000 to 2000 ppm. The average sensitivity of the film sensor was found 1.8 and its response and recovery times were found 50 and 350 sec., respectively. Thus, Cu/Pd nanostructures possess excellent sensing towards the LPG. The sensor based on Cu/Pd nanostructures is user friendly, robust, cost effective and easy to fabricate [55].

Sonker *et al.* obtained that Nanostructured ZnO-MWCNTs was successfully prepared. The crystallite dimension was found 28.43 nm. ZnO-MWCNTs complex sensor showed better sensing response as well as sensitivity at 61.57 and 41.95 respectively [56].

Nakate *et al.* found the LPG sensing response of Au sensitized SnO_2. The Au sensitization and SnO_2 were have prepared by spray pyrolysis deposition method. Maximum LPG response found for unsensitized SnO_2 is 28% at 598K temperature

and for Au sensitized SnO_2 is 57% for 780 ppm gas concentration at comparatively low operating temperature at 598K. These sensors exhibit the potential to detect lesser gas concentration compared to the concentration of 1000 ppm of LPG [Permissible exposure Limit (PEL) for LPG as specified by NIOSH and OSHA standards] with high sensing response. Present results show that Au sensitized SnO_2 have a remarkable LPG sensing properties, which makes it promising high gas response sensor material for combustible gases in practical applications [57].

Nakate *et al.* found that ZnO nanorods have grown on glass substrate by spray pyrolysis deposition (SPD) method using zinc acetate solution. The LPG sensing was extremly improved by sensitization of Au surface noble metal on ZnO nanorods film. Maximum LPG response of 21% was declared for 1040 ppm of LPG, for pure ZnO nanorods sample. After Au sensitization on ZnO nanorods film sample, the LPG response time of 50 sec. The sensor has good stability and hence can be used in effective LPG sensor devices. Unlike in case of CdO containing Cd toxic material, ZnO is co-friendly and stable material for gas sensing application [58].

Singh *et al.* investigated barium titanate composite synthesized through sol-gel technique as well as 1film was formed by whirl fabricating method. Optical characterization results in band gap at 3.9 eV. Peak at 540 cm-1 inveterate the development of $BaTiO_3$. The maximum sensitivity was found as 3.5. The $BaTiO_3$ established LPG sensor is fairly appropriate in the development of profitable LPG sensor [59].

Choudhary *et al.* observed that polypyrrole nanocomposites were prepared in situ route and appealed for LPG. LPG sensing characteristics were crucially concerned by doping with Ag_2O in nanocomposites. It indicates greater sensing response, selectively and stability against LPG. All nanocomposites reported high selectivity towards LPG than CO_2 gas [60].

Chaudhary *et al.* reported that ZnO nanorods were effectively prepared by chemical colloidal method. The LPG response was conceded out for stumpy gas congregation (20-100 ppm) for different operating temperature (120-200℃). The ZnO synthesized by 3 hrs. of refluxing denotes brilliant sensitivity as well as repeatability close to

LPG. Dynamic sites in vacant configuration enhance sensitivity. Thus, hollow ZnO rods are used as well-organized LPG sensor. [61].

Lersak *et al.,* fabricated alcohol gas sensor from thin film SnO_2. The alcohol sensor formed by evaporating titanium and platinum on SnO_2 film at 600℃ in nitrogen atmosphere for 2 hours using an electron beam evaporator. The prepared alcohol sensor detect alcohol concentration up to 10% v/V. Hence, it is used to measure alcohol concentration in commercial wines [62].

Khan *et al.,* provided a circumstantial over view of preparation, features as well as implementation of NPs. They were characterized by SEM, TEM and XRD. Heavy metals NPs of Pb, Hg and Sn were noted to be so rigid and stable [63].

Bonadium *et al.,* synthesized SWCNTs and MWCNTs using Fe and Mo catalysts and MgO as a catalyst support by Catalytic Chemical Vapour Deposition method. The characterization of catalyst was done using X-ray diffraction, SEM, TEM, DTA, TGA as well as Raman spectroscopy. Thermal analysis showed great dispersion in the diameter of MWCNTs due to presence of amorphous carbon. SEM indicated that very fine fibers having diameters below 1 µm. Raman spectroscopy investigated that quality and yield of production [64].

CHAPTER-IV

EXPERIMENTAL PROCEDURE AND CHARACTERIZATION TECHNIQUES

The experimental procedure can be classified in to 6 different steps:

a) Starting materials

b) Oxidation and purification of MWCNTs

c) Substrate preparation

d) Electrophoretic deposition process

e) Application in LPG sensing

4.1 Starting Material:

MWCNTs which were prepared through chemical vapor deposition technique were procured from ILJIN Nanotech. Company Ltd South Korea (purity >98%), used in this work. SDS from HI-Media Laboratory Pvt. Ltd. (Mumbai) India. Concentrated HNO_3, NaOH, Na_3PO_4 and Na_2CO_3 were used from laboratory.

4.2 Oxidation and Purification of MWCNTs

During the synthesis of MWCNTs, some impurities may contain amorphous carbon, fullerenes, nanocrystalline graphite as well as transition metals that are used as catalyst throughout production. These impurities sometimes may hinder the precise examination of MWCNTs features and checks the best presentation of MWCNTs applications to modern functional device. So, they were purified before further treatment. Here, acid refluxed technique was applied for oxidation of MWCNTs. The principal aim of this method was the replacement of metal catalyst, amorphous carbon with inclusion of different oxygen functional groups like -COOH, OH^-, COO^- etc. on the surface. Additionally, the MWCNTs functionalized in such method are

soluble in different solvents due to hydrophobic quality of MWCNTs is restored to hydrophilic because of attachment of polar groups [65].

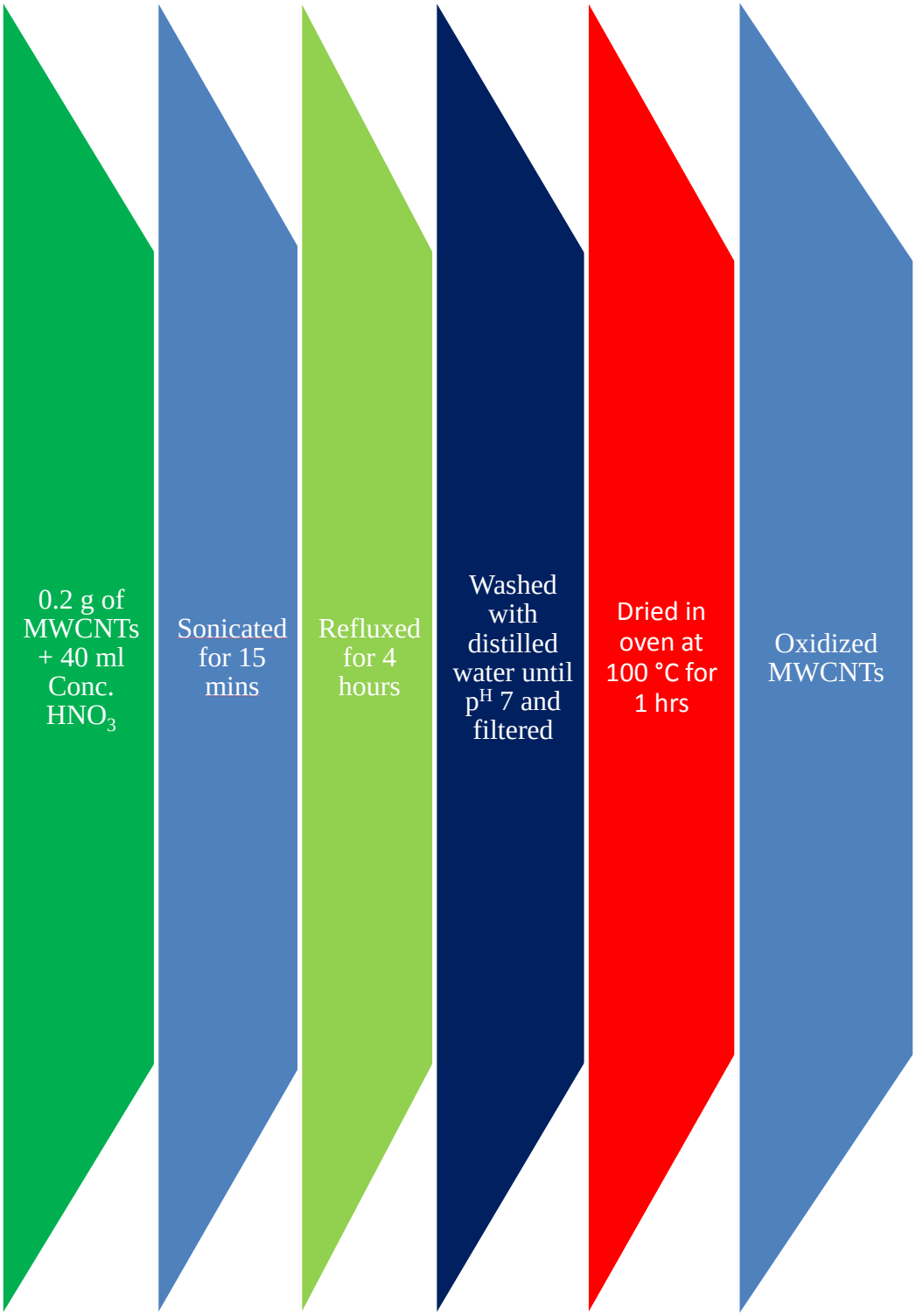

Fig. 4.2 (a) Oxidation of Multi-walled carbon nanotubes through acid reflux Process

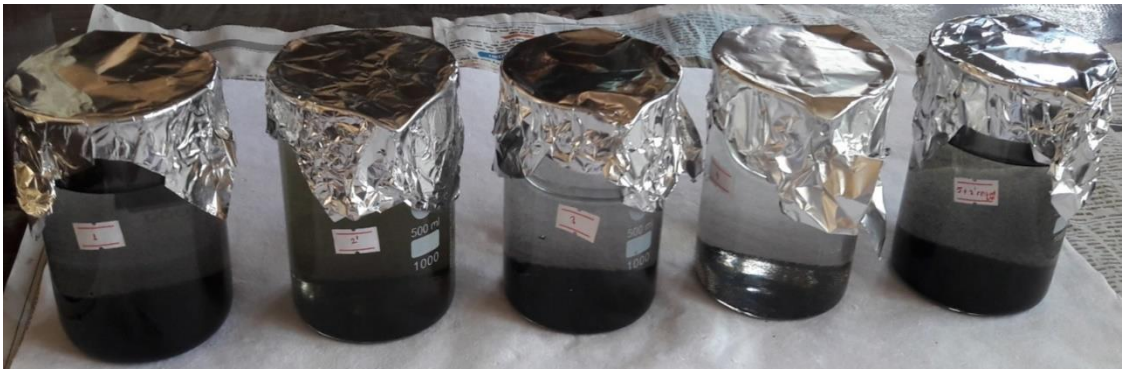

Fig. 4.2 (b) Purification of oxidized Multi-walled carbon nanotubes through decantation methods.

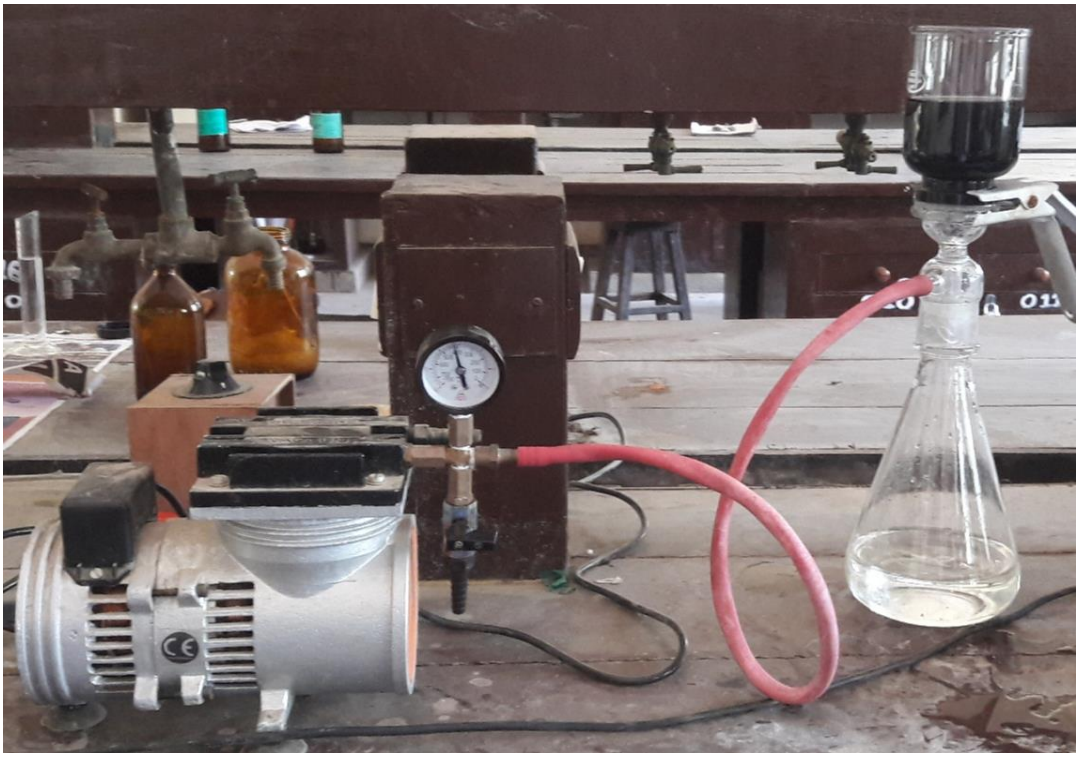

Fig 4.2 (c) Purification of oxidized Multi-walled carbon nanotubes using Suction pump

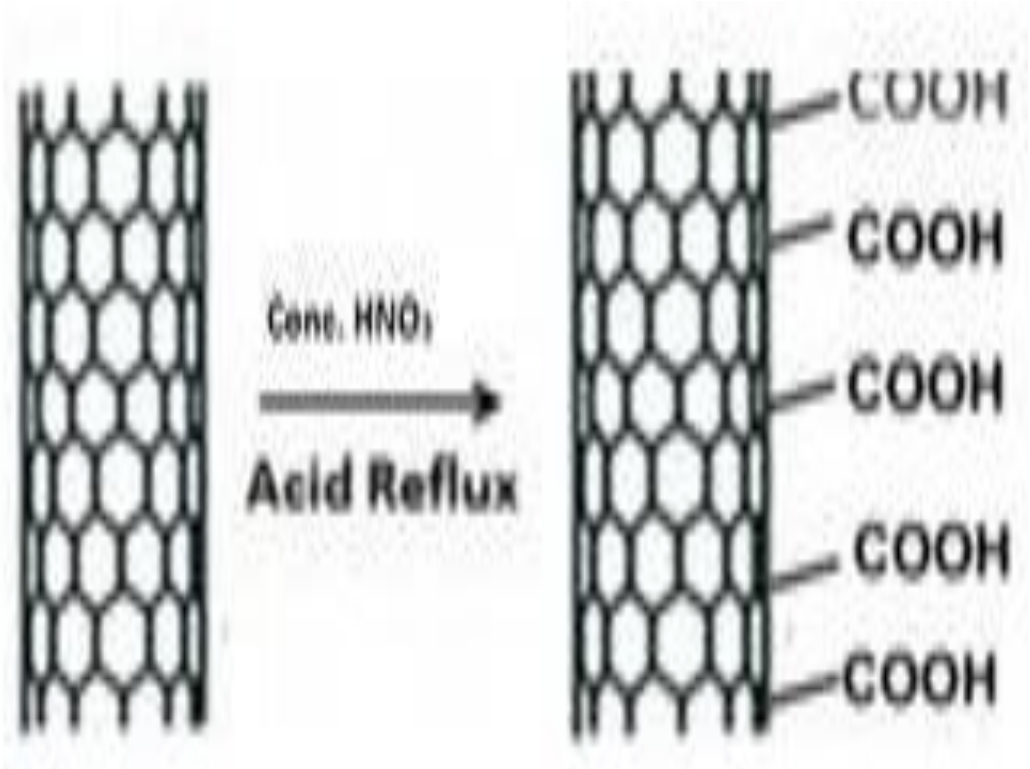

Fig. 4.2 (d) Schematic representation of formation of oxidized MWCTs

In this method, 0.2 g MWCNTs were taken in a round bottom flask and 40 mL conc. HNO_3 was added, then it was sonicated for 15 mins. Then same solution was refluxed for 4 hrs. Then cleaned with distilled water up to p^H 7. Finally, filtered with the help of membrane filter paper with slit size 0.2 micro-meter. Final black residue was then collected, dried in oven at 100^0C for 1 hour [66]. These interactions could be enhanced if structural Nanotubes surface defects or oxygenated oxide layers are present [67].

4.3 Substrate Preparation

Stainless steel was used for the electrophoresis process. In this process, the stainless steels substrates were cleaved into 1 cm in length and 0.5 cm in wide. Before EPD, the plates were degreased with silicon carbide paper ranging upto number 1000, 1500 and 2000, then sonicated for 15 mins. and then dipped into the NaOH, Na_3PO_4, Na_2CO_3 at 60-80^0C till 15 min. Dipped in aqua-regia for 90 seconds. Finally, the plates were cleaned with D. I. water then dried in oven for 10 minutes [68].

Fig; 4.3 Electrophoretically Deposited Substrate

4.4 Electrophoretic Deposition Process

Oxidized MWCNTs were used for the EPD process. For this, oxidized MWCNTs (0.027 g) were immerged in 30 mL D. I. water. These solutions were kept in separate bottles. Then 45 mL 1% SDS were added to each for well dispersion of MWCNTs and then sonicated for 6 hrs.

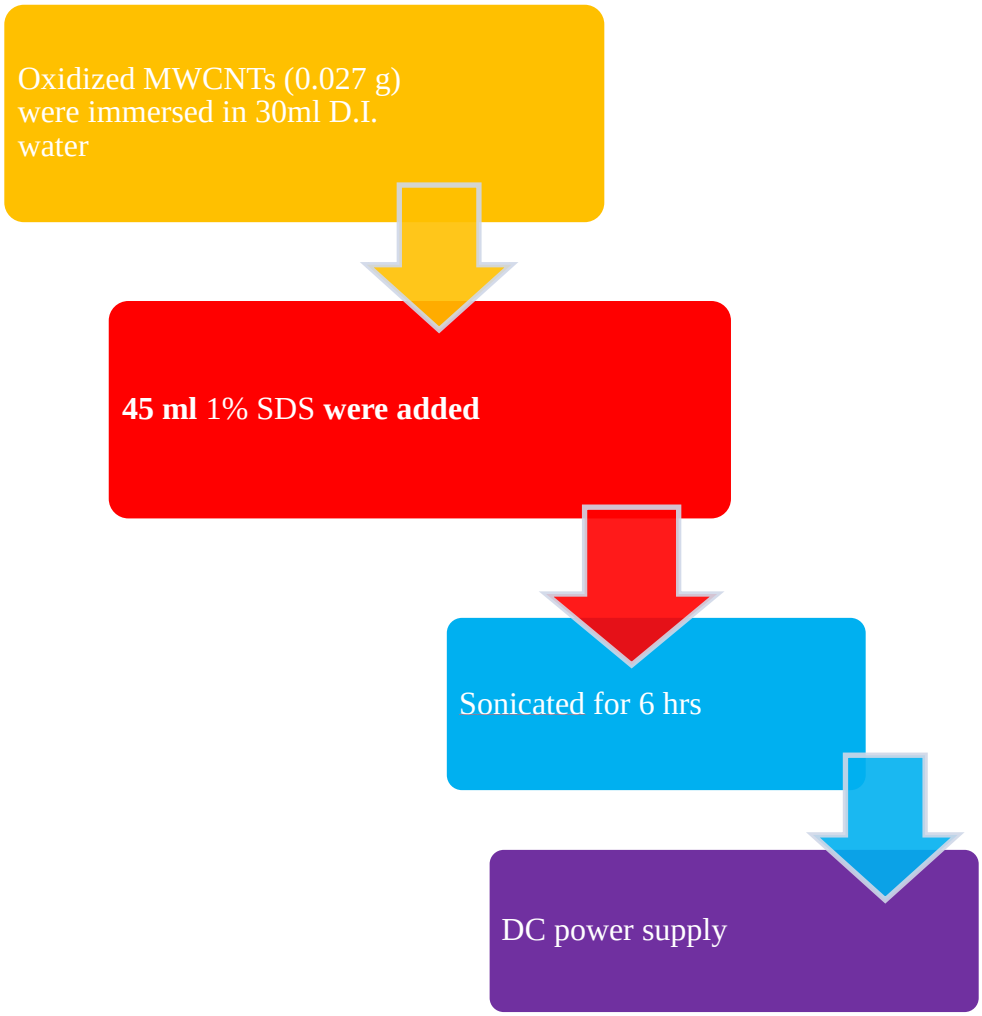

Fig; 4.4 (a) Well Dispersed MWCNTs Solution

The electrophoresis process was performed in an experimental setup consisting of a DC power supply, electrolytic baths and two electrodes, one of which was the substrate for MWCNTs coating. Here, two steel plates were made anode and cathode. They are separated by 1.5 cm for all experiments. The process was carried out for the constant time of 10 minutes using 10V.

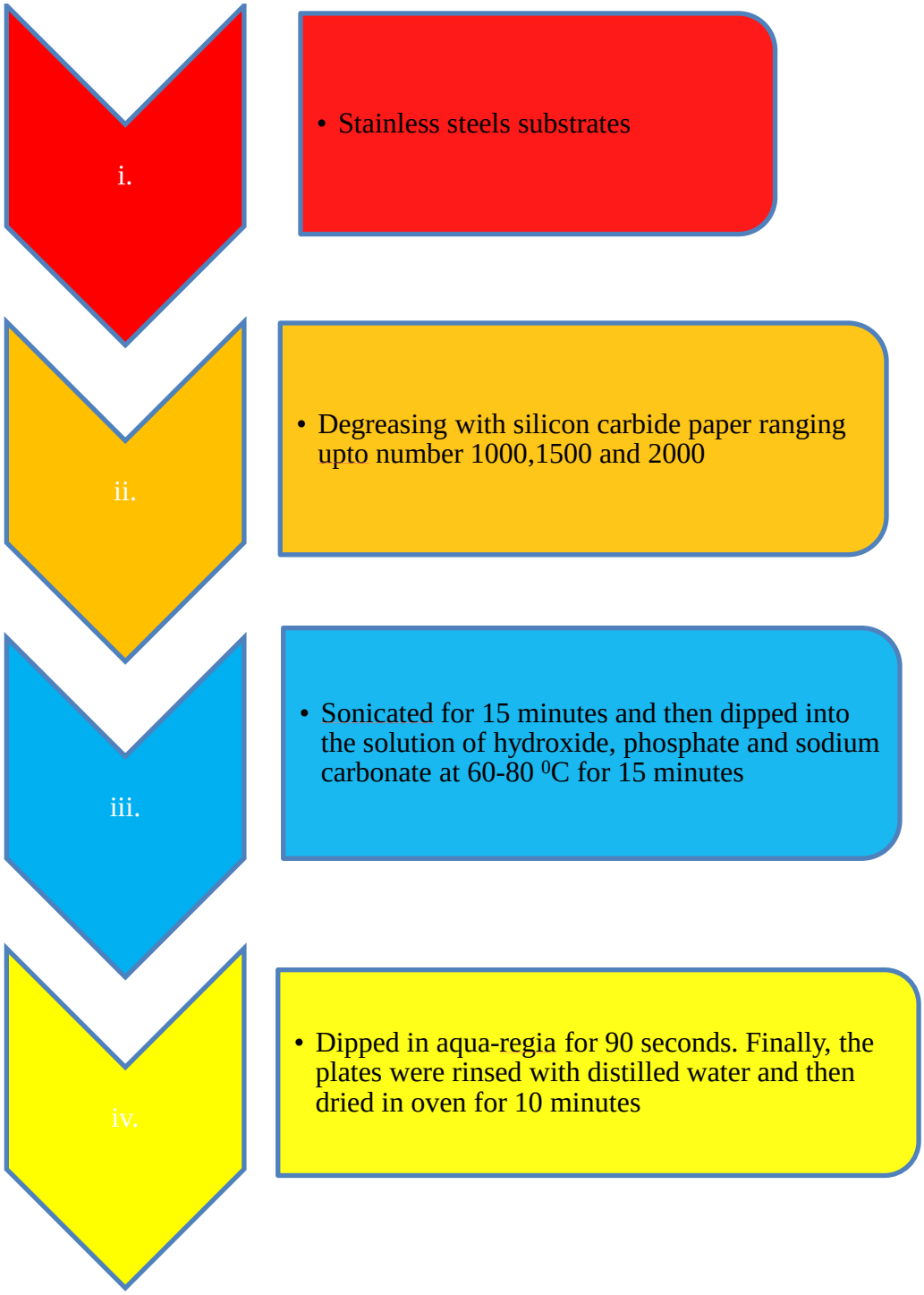

Fig: 4.4 (b) Deposition of Oxidized MWCNTs on stainless steel plate at 10V for 10 min.

Following the deposition process, the samples were carefully taken out of the solution and dried in oven for 24 hrs.

Fig: 4.4 (c) EPD process

4.5 Application in LPG Sensor

For the measurement of electrical resistance, a sealed glass chamber was used. The glass chamber was tightly attached with rubber socket to stop in and out of the air. In glass chamber, a small 4/4 cm of plywood board was also taken with two screws

where electrophoretically deposited substrate was placed in a fixed position. In the glass chamber, one-one holes were created in right and left side were fitted with corks. The main purpose of the hole was in and out of the LPG under test. The resistance was measured by digital multi-meter. The whole set up for measuring sensitivity of the gas is given below.

Fig.4.5 Experimental set up for LPG Sensor

4.6 Characterization Techniques

4.6.1 Infrared Spectroscopy

It reclines allying the visible and microwave part. They have wavelength greater than visible and smaller than microwaves. This technique is used to identify functional group by analysis of their constituent band position. It is classified as;

a. Near-IR (overtone region) 0.7-2.5 µm (14000-1000 cm^{-1})

b. Middle-infrared (vibration-rotation) 2.25-25 µm (4000-400 cm^{-1})

c. Far-infrared (rotation region) 25-1000 µm (400-10 cm^{-1})

The information and its purity can be analyzed by this method.

4.6.2 Scanning Electron Microscopy

It is a technique to gives metaphors of trial by examining the exterior with a focused ray of electrons. The electrons interrelate among atoms inside the trial, giving different signs so as to have detailed about the exterior scenery as well as constitution of prototype.

4.6.3 Raman Spectroscopy

The method used to determine vibrational, rotational and further states in molecular systems, able of exploring the chemical component of substances. It computes comparative frequencies unlike IR spectroscopy.

CHAPTER-V

RESULTS AND DISCUSSION

5.1 FTIR Spectroscopy

MWCNTs was successfully oxidized and purified by acid reflux method. The oxidation of MWCNTs was ensured by FTIR characterization.

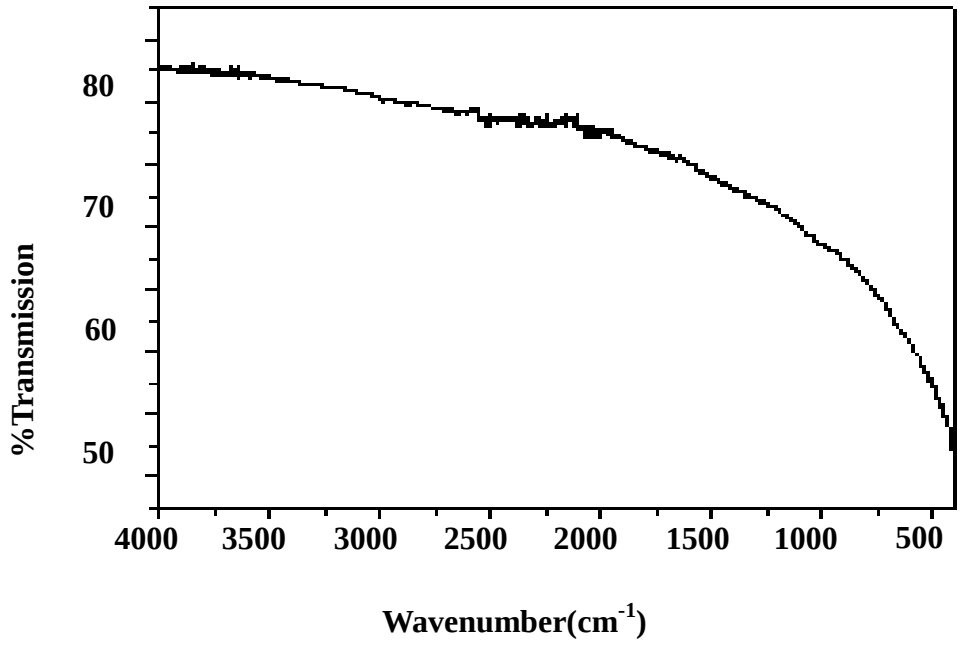

Fig. 5.1(a) FTIR scale of pristine MWCNTs sample

Fig. 5.1(a) shows the IR spectrum of Pristine MWCNTs. The spectrum does not show any sharp infrared peaks, it means it may not contain any functional groups.

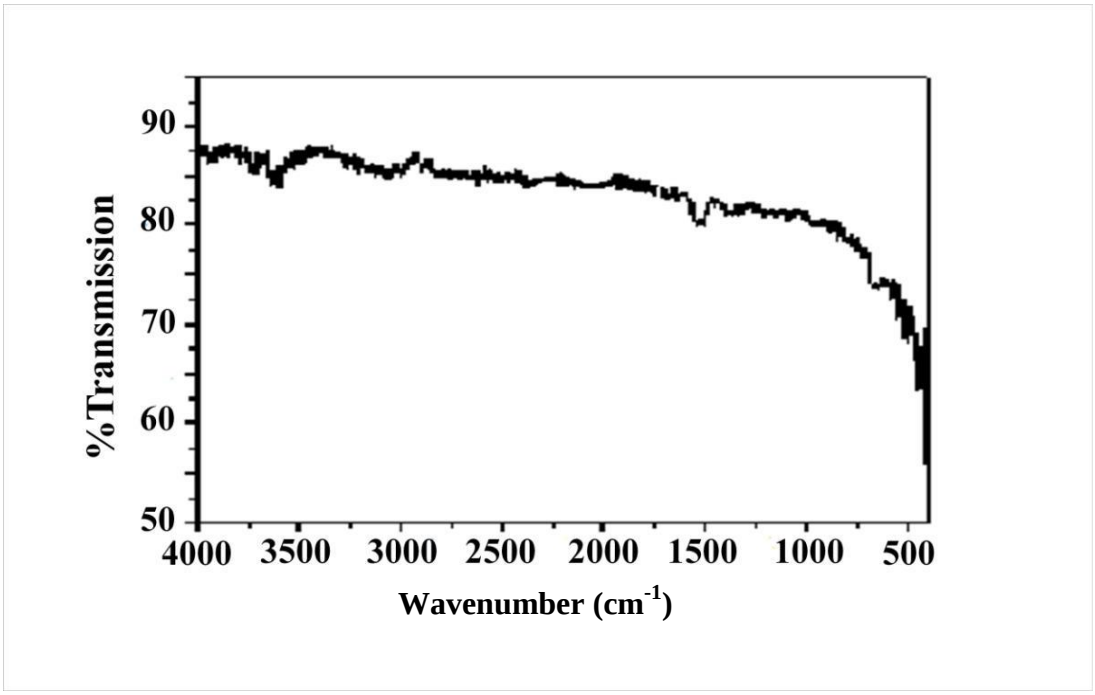

Fig.5.1 (b) FTIR spectrum of Oxidized MWCNTs sample

Fig. 5.2 depicts FTIR spectrum of oxidized MWCNTs. Various changes are seen between the FTIR spectrum of pristine MWCNTs and oxidized MWCNTs. The peak around 3600 cm^{-1} may be due to OH^-group, because the oxidized MWCNT is hydrophilic in nature. The peak located around the 1600 cm^{-1}assigned as carbonyl (C=O) groups. This confirms the presence of oxygen functional group after treatment with acid.

5.2 Scanning Electron Microscopy

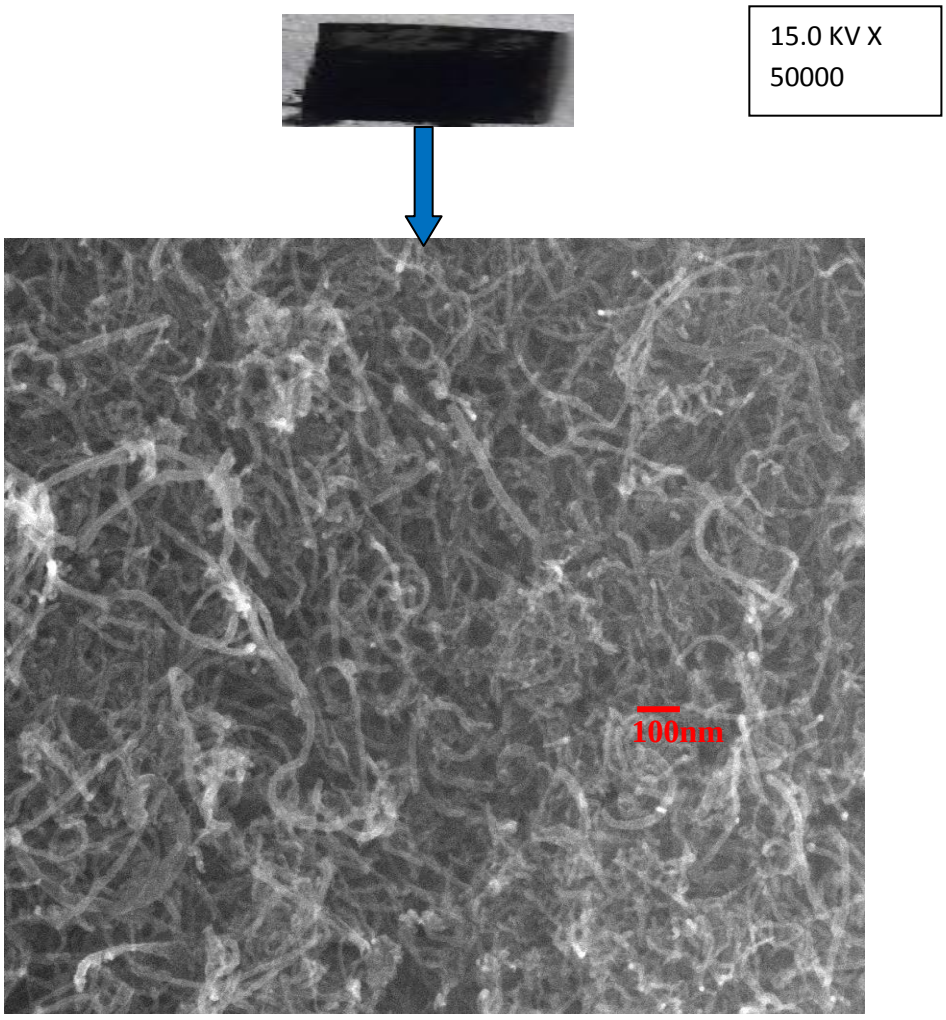

Fig. 5.2 SEM image of oxidized MWCNTs deposited on stainless steel plate

Fig. 5.2 showed the Electrophoretically Deposited Oxidized MWCNTs on stainless steel substrate. The image shows that the MWCNTs deposited with detectable homogeneity and excellent packing density. Uniform and evenly distributed oxidized MWCNTs were observed, as reported by Thomas *et al.*, [68].

5.3 Raman Spectroscopy

Oxidized MWCNTs was profitably coated on stainless steel by electrophoretic deposition method as well as investigated through Raman spectroscopy.

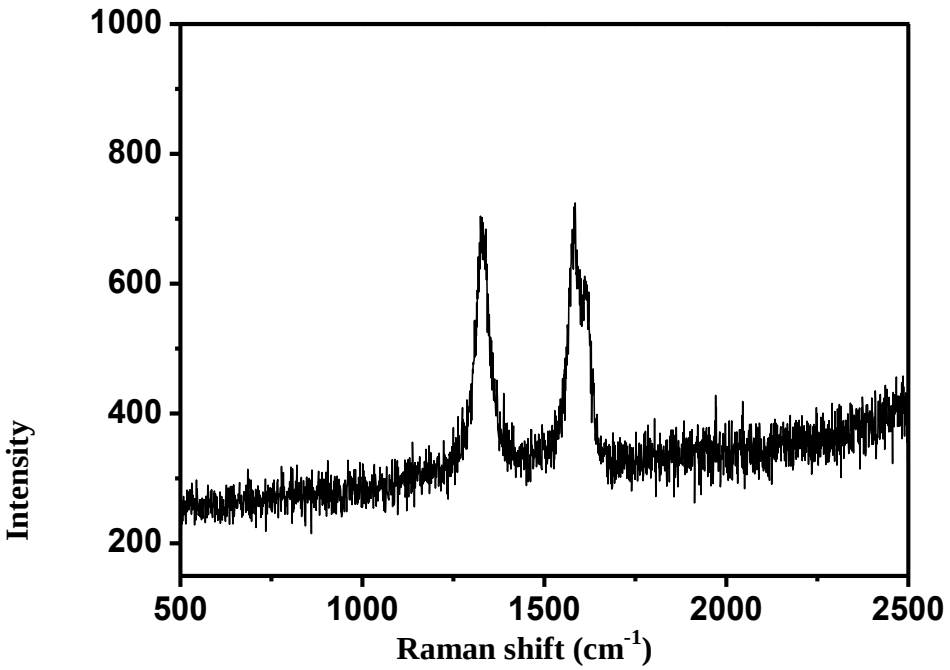

Fig.5.3: Raman spectrum of oxidized MWCNTs

Figure 5.3 indicates the Raman spectrum of electrophoretic deposited MWCNTs. The spectrum shows two characteristic peaks of MWCNTs. The peak at 1570 and 1343 cm^{-1} are G and D-band respectively The G-band is due to sp^2 carbon atoms or it corresponding to the crystallite graphitic structure in the CNT. The D-band is due to disorder in the CNTs.

5.4 Sensing response of MWCNTs on LPG Sensors

If LPG gas chemisorbed, electrical conductivity of MWCNTs is altered. The sensing operation of CNTs gas sensors entails charge transfer. This interconnection alters the conductivity of CNTs. The resistance of MWCNT is changed on exposition to LPG. So, electrons are conveyed from LPG gas molecules to CNTs. LPG molecules donate electrons to form a space charge region (depletion region) on the semiconducting CNT surface. This depletion region decreases the holes transport, thereby changing the electrical resistance of CNTs. The LPG sensing properties were studied by

keeping test sample in a sealed glass chamber. The electrical resistivity electro deposited sample in absence of LPG was recorded (i.e., R_a). Then LPG was passed into the chamber and electrical resistivity of the sample was measured (i.e. R_g). MWCNTs is 'p' type of semiconductor materials and resistance decreases when expose to LPG, the reducing gas [69].

For 'p' type material, sensitivity is calculated by using the formula [70].

$$S\ (\%) = \frac{R_{gas} - R_{air}}{R_{air}} \times 100$$

Where, R_a : resistance of air

R_g : resistance of test gas at a given temperature

S = Sensor Response

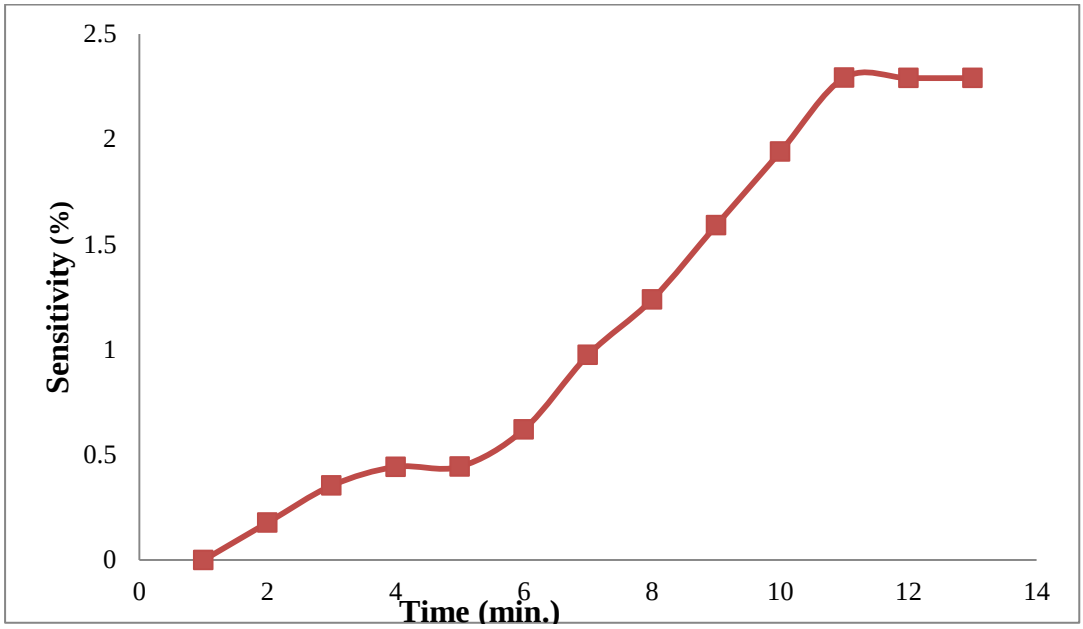

Fig. 5.4 Sensitivity (%) Vs time for 10V for 10 min.

Figure shows that if LPG chemisorbed on CNTs substrate, material suits quite sensitive to gas. Then, sensitivity increases with time then reaches a saturated value after defined time.

The sensitivity is enhanced by operating with NPs. Selective sensitivity to various gases can be verified by deposition of NPs. The sensitivity can be enhanced by doping

Pd on CNTs [70]. Here, oxidized MWCNTs were used to explore the effect of it on interaction with LPG sensor.

5.5 Liquefied Petroleum Gas Sensing Mechanism

Prior to the elucidation of LPG, cubicle was permit to fix at ambient temperature as long as half an hour. The sensing mechanism of the reducing gas (electron donors) like LPG results from the chemical reaction between LPG molecules and the surface of MWCNTs and relates to change in electrical properties of the samples, as discussed in many reports [43, 71]. For example, LPG sensing of the p-type semiconductor has been shown to be p-type sensing properties due to decrease in resistance when exposed to LPG [72]. In air, oxygen molecules in the normal air absorb continuously on the empty absorption sites CNTs, which can be explained by the following equations:

$O_{2(g)} \rightarrow O_2(ads)$ …….(i)

$O_2(g) + e^- \rightarrow 2O^-(ads)$…….(ii)

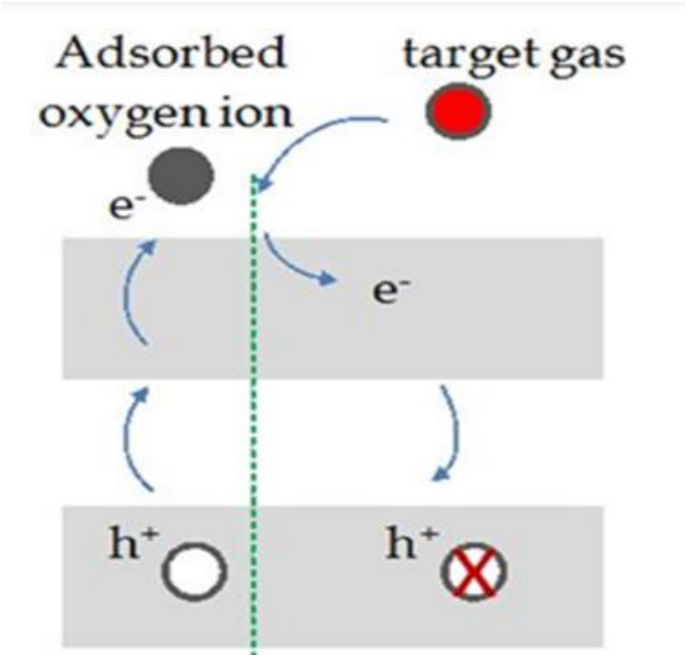

Fig. 5.5 : LPG sensing Mechanism

CNTs generally show p-type properties under normal conditions. By exposing sensor in air, O_2 molecules are chemisorbed on oxidized MWCNTs. It traps electrons from the conduction band and produces negatively charged adsorbed oxygen species such as O_2^- and O^- respectively. Hence, resistance reduces by enhancing holes in conduction band.

$$C_nH_{2n+2} + O_2^- \rightarrow C_nH_{2n}O + H_2O + e^-$$

C_nH_{2n+2} denotes different hydrocarbons. By production of the electrons, the resistance reduces gradually and ultimately set off soaked. If proceed of LPG is cut, O_2 molecules will be soak up on substrate. Hence, sensitivity of sensor increases. The receptor function is an capacity to adsorbed O_2^- charged particle.

CHAPTER-VI

CONCLUSIONS

The dissertation was undertaken with the aim of Electrophoretic Deposition of Oxidized MWCNTs on stainless steel substrates in order to observe the sensor response of deposited materials. Oxidation and purification of MWCNTs was successfully conducted by using conc. HNO_3 solution through acid refluxing method and deposition of MWCNTs were also done by wet chemical method by using ethylene glycol. To identify oxygenated functional group was characterized with the help of FTIR techniques. It is noted that major functional group is carboxylic group and hydroxyl group generated by refluxing. which is absent in pristine MWCNTs.Oxygenated functional groups on the surface of MWCNTs is advantageous for better deposition on the surface of stainless steel.

The uniform EPD of MWCNTs on stainless steel was performed at 10V at constant time 10 min. and a fix electrode distance of 1.5 cm which were analyzed by SEM. Measurement of electrical resistance and sensitivity via closed glass chamber using LPG as targeted gas. MWCNTs were effectively developed above the stainless steel film with CNTs to coat gas sensor. It was sensitive towards LPG at a vast range. MWCNTs were coated on stainless steel to improve sensitivity as well as selectivity of sensors. It was observed that the rate of sensitivity increase with decrease of resistance by EPD with oxidized MWCNTs on stainless steel plate at 10V for 10 min.

REFERENCES

1. Ghorbani H. R., *orient. J. Chem*.,**2015**, *31* (1), 303-305.

2. Tolochko N.K., *His. of Nanotech., ELOSS*, **2009**.

3. Barui A.K., Kotcherlakota R., Patra C.R., *Biom. Appl. of Zinc Oxide Nanoparticles; Elsevier Inc*., **2018**.

4. Khan I., Saeed K., Khan I., *Arab. J. Chem*., **2017**.

5. Muhammad M., Siti S. Mat Isa.,**2015**, 1146-1150.

6. Sola A., Bellucci D., Cannillo V. and Cattini A., *Surface Eng.*,**2011,** 27-28.

7. Gurrappa I. and Binder L., *Sci. Technol. Adv. Mater*., **2008**, *9*, 043001.

8. Boccaccini. A.R., *Composites Science and Eng.*, **2013**, *10*, 208-256.

9. Sarkar P. and Nicholson P.S., *J. Am. Ceram. Soc.*,**1996**, *79*, 1987-2002.

10. Gani M.S.J., *Industrial Ceramics*, **1994**, *14*, 163-174.

11. Zhitomirsky I., *J. Europ. Ceram. Soc.*,**1998**, *18*, 849-856.

12. Boccaccini A.R., Cho J., Roether J.A., Thomas B.J.C., Shafferr M.S.P., *Carbon*,**2006**, *44*, 3149-3160.

13. Heavens N., *Adv.Cem. Process. Technol***., 1990**, *1*, 255-283.

14. Powers R.W., *Electrochem. Soc*., **1975**, *122*, 482-486.

15. Ferrari B., Moreno R.J., *Eur. Ceram. Soc*., **1997**, *17*, 549-556.

16. Greenwood R., Kendall K., *J. Eur. Ceram. Soc.*,**1999**,*19*, 479–488.

17. Fraczek-Szczypta A., Dlugon E., Weselucha-Birczynska A., Blazewicz M., *J. Mole. Struct.*,**2013**, *1040*, 238-245.

18. Wang Y.C., Leu C., Hon M.H., *J. Am. Cem. Soc*., **2004**, *87*, 84-88.

19. Basu R.N., Randall C.A, Mayo M.J. *Am. Cem. Soc*., **2004**, *84*, 33-40.

20. Peng Z., Liu M., *J. Am. Cem. Soc*., **2001**, *84*, 2838.

21. Suresh S., Mortensen A. *Intl. Matter. Rev.*,**1997**,*42*, 85-116.

22. Bueno S., Baudin C., *J. Eur. Cem., soc*., **2007**, *27*, 1455-1462.

23. Vandeperre L., Biest OVD., Clegg W., *Key Eng. Matte*.,**1997**,*1*,127-131.

24. Basu. R., Randall C., Mayo M., *J. Am. Cem. Soc*., **2001**, *84*, 33-40.

25. Yadav B. C., Singh S., and Yadav A., *J. Applied Surface Science*,**2011,***257*, *6*, 1960– 1966.

26. Tomas B. and Skariah B., *J. Alloys and Compounds*., **2015**, *625*, 231–240.

27. Pourfayaz F., Khodadadi A., Mortazavi Y., and Mohajerzadeh S.S., *J. sensors and Actuators B: Chemica.*,**2005**, *108*, 172–176.

28. Bulakhe R.N., Patil S.V., Deshmukh P.R., Shinde N.M., and Lokhande C.D., *J. Sensors and Actuators B: Chemical*, **2013**, *181*, 417–423.

29. Talwar V., Singh O., and Singh R. C., *J. Sensors and Actuators B: Chemical*, **2014**, *205*, 102–110.

30. Singh S., Gupta V., Yadav B. C., Tandon P., and Singh A. K., *J. Sensors and Actuators B: Chemical*, **2014**, *195*, 373– 381.

31. Haridas D., Chowdhuri A., Sreenivas K., and Gupta V., *J. Sensors and Actuators B:* Chemical, **2011**, *153*, 152–157.

32. Dhawale D. S., Salunkhe R. R., Patil U. M., Gurav K. V., More A. M., and Lokhande C., *J. Sensors and Actuators B: Chemical*, **2008**, *134*, 988–992.

33. Sen T., Shimpi N. G., Mishra S., and Sharma R., *J. Sensors and Actuators B: Chemical*, **2014**, *190*, 120–126.

34. Barkade S.S., Pinjari D.V., Nakate U.T., *Chemical Engineering and Processing: Process Intensifcation*, **2013**, *74*, 115–123.

35. Vuong N. M., Chinh N.D., Huy B.T., and Lee Y.I., "*Scientific Reports*, ***2016***, *6*, 26736-26745.

36. Wei B.Y., Ming-Chih H., Hong-Ming L., Ren-Jang W., Hong-Jen L., *J. Sensors and Actuators B: Chemical*, **2004**, *101*, 81–89.

37. Bittencourt C., Felten A., Espinosa E. H., *J. Sensors and Actuators B: Chemical*, **2006**, *115*, 33–41.

38. Kumar S., Rani R., Dilbaghi N., Tankeshwar K., Kim K.H., *Chem. Soc. Rev*, **2017**, 158–196.

39. Dzepina B., Sigalas I., Herrmann M, Nilen R., *Hard. Mater*, **2013**, 36, 126-129.

40. Dzepina B., Sigalas I., Herrmann M., Nilen R., *Int. J. Refract. Met. Hard. Mater.*, **2013,** 36, 126-129.

41. Chiu W., Lee K., Hsieh W., *J. Power sources*, **2011**, 196, 3683-3687.

42. Machappa T., Sasikala M., and Ambika P., *J. IEEE Sensor*, **2010**, 10, 414-419.

43. Yudianti R., Onggo H., Sudirman, SaitonY., Iwata T., Azuma J., *J. open Matter. Sci.***2011**, 5, 243.

44. Kasim S. H., Hashim A. H., *J. Indust. Techno,***2010,***19* (1), 139-148.

45. Dangi P., Bhatt J.P., Shrestha S., 2018, *04* (*07*), 30–34.

46. Liu Y.L., Yang H.F., Yang Y., Liu Z.M., Shen. G.L., *J. thin solid films*, **2006**, 497, 355-360.

47. Arindam G., Ramphal S., Anil G., Vidya S.T., Rajesh A.J., Dipalee J.D., Yuvraj G., Jadhav K.M., Sung-Hwan H., *J. Sensors and Actuators B.*,**2010,** 146, 69–74.

48. Arindam G., Ramphal S., Anil G., Vidya S.T., Rajesh A.J., Dipalee J.D., Yuvraj G., Jadhav K.M., Sung-Hwan H., *J. Sensors and Actuators B.*,**2010,** 146, 69–74.

49. Sivapunniyam A., Wiromrat N., Myint Z., Joydeep D., *J. Sensors and Actuators B.*,**2011,** 157, 232–239.

50. Patil L.A., Shinde M.D., Bari A.R., Deoa V.V., Patil D.M., Kaushik M.P., *J. Sensors and Actuators B.*, ***2011***, 155, 174–182.

51. Gurav K.V., Patil U.M., Shin S.W., Pawar S.M., Kim J.H., Lokhande C.D., *J. Alloys and Compound*, ***2012***, 525, 1–7.

52. Singh S., Singh A., Yadav B.C., Dwivedi K., *J. Sensors and Actuators B.*,**2013**, 177, 730–739.

53. Ravikiran Y.T., Kotresh S., Vijayakumari S.C., Thomas S., *J. Current Applied Physics.*,**2014,** 14, 960-964.

54. Patil Pallavi T., Anwane Rajshri S., Kondawar Subhash B., *J. Procedia Materials Science.*,**2015**, 10, 195 – 204.

55. Jaiswal A., Singh S., Singh A., Yadav R.R., Tandon P., Yadav B.C., *J. Mater. Chemistry and Physics.*,**2015**, 154, 16-21.

56. Sonker R.K., Singh M., Kumar U., Yadav B. C., *J. Inorg. Organomet Polymer.*, **2016**, 31, 1434-1440.

57. Nakate U.T., Patil P., Ghule B., Ekar S., Jadhav V.V., Mane R.S., Kale S.N., *J. Anal. Appl. Pyrolysis.*,**2016**, 27, 29-35.

58. Nakate U.T., Bulakhe R.N., Lokhande C.D., Kale S.N., *J. Appli. Surface Scie.*,**2016**, 371 224–230.

59. Singh M., Yadav B.C., Ranjan A., Kaur M., Gupta S.K., *J. Sensors and Actuators B.*, **2017**, 241, 1170–1178.

60. Choudhary A.R., Waghuley S.A., *J. Mater. Lette.*,**2017**, 26, 253-258.

61. Chaitongrat B. and Chaisitsak S., .*J. Nanomaterials.***, 2018**, 11, 44-50.Jabeena M., Iqbalb A., Kumar R., Ahmed M., *J. Sensing and Bio-Sensing Research***, 2019**, 25, 235-293.

62. Promsong L., Sriyudthsak M., *Sensor And Actuators*,**1995,** B 24-25, 504-506.

63. Khan I., Saeed K., Khan I., *Arab. J. Chem.*,**2017**.

64. Bonadiman R., Lima M.D., Andrade M. J., *J Mater Sci*, **2006,** *41*, 7288-7295.

65. Yi-Qi w., Byum J.H., Kim B.S., Song J., *J. Cent. South University*, **2012**.19, 3017-3022.

66. Ramirez J.M. O., Cornelio M.L.C., Godinez J.U., Arco E. B., Castellanos R.H., *J. hydrogen energy*, **2007**, 32, 3170-3173.

67. Lin L.Y., Wu Y.S. Chang C., Tseng F.G., *J. Physics*., **2013**, 476.

68. Fraczek-Szczypta, Dlugon E., Weselucha-Birczynska A., Nocun M., Blazewicz M., *mole. struc*.,**2013**, 1040, 238-245.

69. Nguyen L., Phan P., Duong H., Nguyen C., *Sensors*,**2013**, 13, 1754-1762.

70. Thomas B. J. C., Boccaccini A.R., Shaffer M.S.P., *J. European Ceramic Society*, **2005**, 25, 1515–1523.

71. Kong, J., Chapline M.G., Dai H., *J. Adv. Mater*. **2001**, 13, 1384–1386.

72. Jadhav V. V., Patil S. A., Shinde D. V., *J. Sensors and Actuators B: Chem.*,**2013**

APPENDIX

The sample which deposited on stainless steel plate at 10 min. by using 10V are taken as follows.

Time (min.)	Sensitivity (~)
0	0
1(on) 1(off)	0.178
2(on) 2(off)	0.354
3(on) 3(off)	0.443
4(on) 4(off)	0.444
5(on) 5(off)	0.621
6(on) 6(off)	0.974
7(on) 7(off)	1.238
8(on) 8(off)	1.591
9(on) 9(off)	1.94
10(on) 10(off)	2.292
11(on) 11(off)	2.290
12(on) 12(off)	2.290